frontiers | Frontiers in Soil Science

TYPE Original Research
PUBLISHED 04 December 2025
DOI 10.3389/fsoil.2025.1718929

OPEN ACCESS

EDITED BY
Genxing Pan,
Nanjing Agricultural University, China

REVIEWED BY
Gyanendra Dhakal,
Saitama University, Japan
Utik Tri Wulan Cahya,
Universitas Tribhuwana Tungga Dewi, Indonesia

*CORRESPONDENCE
Maha Elbana
maha.elbana@agr.bsu.edu.eg

RECEIVED 05 October 2025
REVISED 11 November 2025
ACCEPTED 18 November 2025
PUBLISHED 04 December 2025

CITATION
Elbana M, Gamal R, El-Shirbeny MA, Rashad M, Brouziyne Y and Abou Hadid AF (2025) Mesoporous biochar reshapes soil water dynamics under shallow groundwater: interactions with nitrogen management. *Front. Soil Sci.* 5:1718929. doi: 10.3389/fsoil.2025.1718929

Mesoporous biochar reshapes soil water dynamics under shallow groundwater: interactions with nitrogen management

Maha Elbana[1]*, Rania Gamal[2], Mohammed A. El-Shirbeny[3], Mohamed Rashad[4], Youssef Brouziyne[5] and Ayman F. Abou Hadid[6]

[1]Soil and Water Science Department, Faculty of Agriculture, Beni-Suef University, Beni Suef, Egypt, [2]International Center for Agricultural Research in Dry Areas (ICARDA), Cairo, Egypt, [3]Agricultural Applications Department, National Authority for Remote Sensing and Space Sciences (NARSS), Cairo, Egypt, [4]Land and Water Technologies Department, Arid Land Cultivation Research Institute, City of Scientific Research and Technological Applications (SRTA-City), Alexandria, Egypt, [5]International Water Management Institute (IWMI), Middle East and North Africa (MENA) Office, Giza, Egypt, [6]Faculty of Agriculture, Ain Shams University, Cairo, Egypt

Shallow groundwater tables influence nearly one-quarter of global croplands, yet the role of biochar in such hydropedological settings remains poorly understood. This study investigated how mesoporous biochar interacts with nitrogen fertilization to modify soil properties, water dynamics, and irrigation requirements in a clay loam soil of the Nile Delta, Egypt. A two-season field experiment using randomized complete block design tested biochar (35 t ha^{-1}) combined with three nitrogen levels (100, 80, and 50% of the common farmer practice). Biochar significantly increased available N, Ca, and Mg and altered soil moisture profile: Instead of monotonic moisture increase typical of shallow groundwater conditions, an S-shaped distribution developed within the 0–30 cm layer. Drainage losses consistently declined when biochar was combined with moderate nitrogen input. Although crop yield and fruit quality responses were not statistically significant, the biochar-nitrogen combination reduced irrigation demand by ~82 m^3 ha^{-1} yr^{-1} compared to conventional management. When scaled regionally under same environmental conditions, this strategy could save >80 million m^3 of irrigation water annually in Egypt, assuming 100% irrigation efficiency. These findings show that mesoporous biochar can reshape root-zone water dynamics under shallow groundwater, offering a promising strategy to enhance water-use efficiency in water-scarce regions.

KEYWORDS

soil water retention, water productivity, water savings, fine-textured soil, tomato

1 Introduction

Biochar, a carbon-rich by-product of biomass pyrolysis, is widely studied as a soil amendment for improving fertility, water retention, and soil structure (1–5). Its porous structure enables adsorption of nutrients and water, thereby reducing leaching and enhancing resilience to stresses such as salinity and drought (6–9). However, biochar effects are highly variable, depending on feedstock, pyrolysis conditions, and soil texture, with fine-textured soils often showing weaker or even negative responses compared to sandy soils (1, 10, 11). Recent research has also emphasized that biochar does not consistently improve soil physical properties, especially in fine-textured or clay-rich soils. Hydrophobicity, particle size, and pore structure can limit infiltration and water entry into biochar particles, reducing the expected gains in water retention and aggregate stability (12, 13). In some cases, biochar may decrease pore connectivity or alter cation exchange capacity, thereby restricting aeration and hydraulic conductivity and leading to neutral or even negative effects on soil structure (14, 15).

Most biochar research has been conducted under conventional irrigation and free-drainage conditions. In contrast, shallow groundwater table influence 22–32% of global croplands (16–18), including large areas of the Nile Delta, Argentine Pampas, US Corn Belt, and Western Siberia (19–23). Such hydrological settings affect soil water availability through capillary rise but can also cause waterlogging and salinization (24, 25). Biochar may alter hydraulic conductivity and moisture retention (26, 27), yet its performance under sustained shallow groundwater influence remains poorly understood.

Nitrogen fertilization is another key driver of soil–plant interactions. While essential for crop productivity (28–30), excessive nitrogen contributes to nitrate leaching and greenhouse gas emissions (31, 32). Biochar has the potential to improve nitrogen use efficiency by adsorbing ammonium and nitrate, supporting microbial cycling, and moderating leaching (33–36). Yet, the combined effects of biochar and nitrogen fertilization on soil water dynamics remain largely unexplored in shallow groundwater environments.

Long term studies indicate that biochar undergoes physical, chemical, and biological aging in soil leading to fragmentation and interactions that alter microbial activity and soil structure. Consequently, initial improvements in bulk density, porosity, and water retention may diminish over time, particularly in fine textured soils (37–39). However, most long-term assessments extend for less than a decade, and aging dynamics remain highly site-specific, depending on soil type, climate, and biochar properties. These uncertainties underscore the importance of evaluating how mesoporous biochar influence soil water behavior under field conditions affected by shallow groundwater.

This study addresses this gap through a two-season field experiment in the Nile Delta, Egypt. We tested the hypothesis that mesoporous biochar interacts with nitrogen fertilization to (i) modify soil physical and chemical properties, (ii) reshape soil water dynamics and irrigation requirements under shallow groundwater, and (iii) maintain crop performance while improving water use efficiency. By including a regional scaling analysis, we also evaluate the broader water-saving potential of this management strategy across Egypt and the Middle East and North Africa (MENA) region.

2 Materials and methods

2.1 Site description and baseline soil properties

The field experiment was conducted at the experimental farm of the Arid Lands Agricultural Studies and Research Institute (ALARI), Ain Shams University, Egypt (31.24475° E, 30.116° N, 21 m a.s.l.). The site is characterized by a clay loam soil texture (34.42% clay and 35.92% silt). It has an arid climate with negligible annual rainfall. Weather data were obtained from the ALARI weather station (https://ng.fieldclimate.com). Mean maximum and minimum air temperatures during season 1 (spring 2023) were 33. 5 ± 3.9 °C and 20.2 ± 3.3 °C, respectively, while during season 2 (autumn 2023) they were 26.0 ± 4.9 °C and 15.1 ± 5.1 °C, respectively. The average reference evapotranspiration ranged from 4.0 ± 0.6 mm day^{-1} in season 1 to 1.5 ± 0.5 mm day^{-1} in season 2) Supplementary Figure 1).

Before transplanting, the soil was ploughed and amended with 48 m^3 ha^{-1} compost and 950 kg ha^{-1} calcium sulphate. A commercial corn cob-derived biochar, available in the Egyptian market, was incorporated into the 0–30 cm soil layer of the biochar plots at 35 t ha^{-1} following (40). Following soil bed preparation and biochar incorporation, the field was left undisturbed for one week before transplanting to allow soil physical conditions to stabilize. The biochar was characterized prior to application to determine its surface area and pore structure. Nitrogen adsorption–desorption isotherms were obtained using a BELSORP-miniX analyzer at 77 K. The BET (Brunauer–Emmet–Teller) and BJH (Barrett–Joyner–Halenda) methods (41) were applied to determine surface area pore size distribution. The biochar exhibited a BET surface area of 3.53 m^2 g^{-1}, a total pore volume of 0.0076 cm^3 g^{-1}, and an average pore diameter of 8.56 nm, confirming its mesoporous structure. Full isotherm and pore distribution data are provided in Supplementary Table 2 to ensure transparency and reproducibility. Since the biochar was commercially sourced, specific pyrolysis conditions were not available from the supplier.

2.2 Experimental design and treatment

A randomized complete block design (RCBD) with three replicates was employed (Figure 1). The experiment evaluated the interaction between biochar and application of nitrogen fertilization rate on soil moisture content, crop yield, water productivity, and irrigation water savings. Treatments combined two levels of biochar (absent or applied at 35 t ha^{-1}) with three nitrogen rates corresponding to 100%, 80%, and 50% of the common farmer practice. Accordingly, six treatments were established. Treatment W1: 100%N without biochar (control), W8: 80%N without biochar,

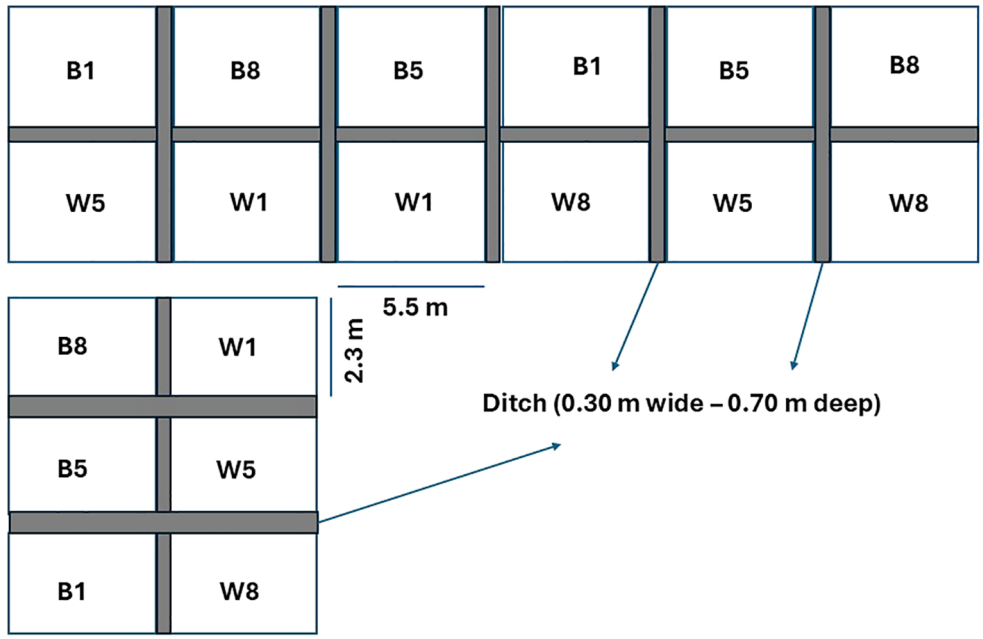

FIGURE 1
Experiment RCBD statistical design. Treatments include biochar amended plots (B1, B8, and B5) and unamended plots (W8, and W5) vs the control treatment W1 (common practice).

W5: 50%N without biochar, B1: 100%N with biochar, B8: 80%N with biochar, and B5: 50%N with biochar. Each experimental plot measured 5.5 m × 2.3 m and was hydraulically isolated using 30cm-wide and 70 cm-deep ditches to prevent lateral movement between plots. All plots were initially irrigated to saturation before transplanting to ensure uniform soil moisture conditions at the start of the experiment.

Nitrogen was supplied as ammonium sulphate and ammonium nitrate in four splits at 15, 50, 70, and 90 days after transplanting (DAT). Seasonal totals were 300, 240, and 150 kg N ha^{-1} for 100, 80, and 50% treatments, respectively. Detailed per-plot rates are shown in Supplementary Table 1. Micronutrients were foliar applied starting 30 DAT and repeated every 15 days until fruit ripening: 0.5 g L^{-1} chelated Zn, Fe, and Mn, and 1.5 g L^{-1} potassium sulphate.

2.3 Irrigation management and soil water monitoring

Irrigation was delivered weekly via a drip irrigation system with a dedicated valve for each subplot. Irrigation water volumes were calculated to restore the root zone field capacity using the following equation.

$$I = (\theta_{fc} - \theta_i) \times A \times Z$$

where I is irrigation water (m^3), θ_{fc} is volumetric soil water content at field capacity, θ_i is volumetric soil water content at irrigation time, A is plot area, and Z is effective root zone depth (m).

The applied irrigation water volume was measured using flowmeter installed on the submain irrigation line.

Volumetric SWC was monitored daily with a TDR (Time Domain Reflectometry) probe (PR2/6, Delta–T Devices Ltd., UK) at depths of 10, 20, 30, 40, 60, and 100 cm. Irrigation scheduling was based on maintaining root zone was considered 0–25 cm during the first 30 days after transplanting and 0–40 cm thereafter. This approach ensured SWC did not fall below 50% of available water, following recommendations for tomato (42).

Calibration was performed by taking soil samples simultaneously with TDR readings. Gravimetric water content was measured in the field laboratory following (43) and volumetric SWC was calculated as gravimetric $SWC \times (bulk\ density/water\ density)$. Calibration equation was derived by linear regression, and model fit assessed using R^2, RMSE, MAE, and residual diagnostics. Because SWC at 100 cm depth was consistently saturated, this layer was considered the shallow water table boundary.

2.4 Crop management, sampling and analysis

Tomato (*Lycopersicon esculentum Mill.*) cultivar K186 (Rich Zoan) seedlings were transplanted in two seasons. Season 1 (spring 2023) ran from 6 April to 9 July; season 2 (autumn 2023) from 25 September 2023 to 23 January 2024. Harvesting was conducted from the central 1 m^2 of each plot to minimize border effects. Fruit samples were analyzed for lycopene, moisture content, and total soluble solids (TSS) following standard procedures (44, 45).

Soil pH and EC were measured in a 1:2.5 soil–water suspension, while total available macronutrients were determined after

extraction/digestion following established protocols (46, 47). Full details and instrument specifications are provided in [(48); Zenodo. https://doi.org/10.5281/zenodo.17195601].

2.5 Soil hydraulic properties

Composite soil samples (0–20 and 20–40 cm) were collected at the start of the experiment. Soil water content at field capacity (≈ −330 cm matric potential) and permanent wilting point (≈ −15, 000 cm) were measured using a pressure plate apparatus (49). Bulk density was determined by the core method (43).

Soil water flux was calculated dynamically using the Buckingham–Darcy law (50, 51) expressed as:

$$q = -K(\theta) \times \left(\frac{dh}{dz} + 1\right)$$

where q is soil water flux (cm day^{-1}), defined as positive for upward capillary rise and negative for downward drainage, $K(\theta)$ denotes the unsaturated hydraulic conductivity (cm day^{-1}), and dh/dz is the matric potential gradient driving water movement.

Water retention characteristics were described using the van Genuchten model (52), with residual (θ_r) and saturated water content (θ_s) estimated from soil bulk density and particle size distribution. The shape parameters α and n were derived from pedotransfer functions based on sand and clay contents, while unsaturated conductivity functions were calculated following (53). For each depth and treatment, time-series of volumetric SWC obtained from calibrated TDR data (θ) is used to compute effective saturation, $K(\theta)$, matric gradients, and resulting fluxes.

2.6 Water productivity and irrigation water savings

Water productivity (WP) was calculated as yield per unit of applied irrigation (54).

$$WP_i = \frac{Y_i}{I_i}$$

where Y_i is yield (kg ha^{-1}) and I_i is applied irrigation (m^3 ha^{-1})

Irrigation water savings relative to the conventional agricultural practice (W1 = 100% N without biochar) was calculated as:

$$WS_t = I_{w1} - I_t$$

where WS_t is mean water saved (m^3 ha^{-1}), I_{w1} is irrigation water for the relative baseline treatment, and I_t mean irrigation water for t treatment.

2.7 Statistical analysis and visualization

All statistical analysis were conducted in R version 4.5.1 (R Core Team, 2024). Descriptive statistics (mean, standard error) were computed for all measured variables.

Tomato yield, fruit quality attributes (lycopene, total soluble solids, fruit moisture), and soil chemical properties (N, P, K, Mg, pH, EC) were analyzed using analysis of variance (ANOVA) within a split-plot RCBD framework. Biochar (with vs without), nitrogen fertilization rate (100, 80, 50% of the recommended dose), and season (spring vs autumn) were treated as fixed factors, and block was included as a random factor. When ANOVA indicated significant effects, pairwise comparisons among treatments were conducted using Tukey's honestly significant difference (HSD) test at $\alpha = 0.05$.

SWC calibration was first calibrated by linear regression of gravimetrically determined volumetric SWC against TDR probe output. Model performance was assessed using the coefficient of determination (R^2), root mean square error (RMSE), mean absolute error (MAE), and residual diagnostics. Repeated SWC observations across depths (10–100 cm) were analyzed wit linear mixed-effects models (packages *Ime4, ImerTest*). Fixed effects included biochar treatment, nitrogen rate, season, and depth, with random intercepts specified to account for repeated measurements within plots. Competing models were compared using Akaike's information criterion (AIC), and the best-fitting model was used to estimate marginal means and perform pairwise contrasts with Tukey adjustment (*emmeans* package). Model assumptions were checked by visual inspection of residual plots and tested formally with the Shapiro–Wilk test for normality and Levene's test for homogeneity of variances. Soil water flux values were summarized by treatment and season, with mean ± standard error reported. Treatment effects were tested using analysis of variance (ANOVA) with biochar, nitrogen rate, and season as fixed factors, followed by Tukey's HSD for pairwise comparisons.

Data visualization was performed using the *ggplot2* package. Boxplots and line graphs were used to display treatment effects on SWC, yield, fruit quality traits, and soil chemical properties, with treatment means and standard errors overlaid. Diagnostic plots (residuals vs. fitted, Q-Q plots) were examined to confirm model assumptions. Full R scripts for ANOVA, mixed models, soil water parameters estimation, and diagnostic figures are provided in [(48); Zenodo. https://doi.org/10.5281/zenodo.17195601] to ensure reproducibility.

3 Results

3.1 Biochar characterization

The adsorption/desorption isotherms, BET and BJH plots for the applied biochar are illustrated in Figure 2. The summary of the physicochemical characterization data for biochar sample via nitrogen physisorption analysis is documented in Supplementary Table 2. The adsorption/desorption isotherms confirmed that the applied biochar was mesoporous, exhibiting a type IVa profile (55). Pore diameter averaged 8.56 nm, with a pore volume of 0.00756 cm^3 g^{-1}, while the BET surface area was relatively low (3.53 m^2 g^{-1}). The hysteresis loop indicated capillary condensation in mesopores, consistent with nitrogen physisorption patterns (41). Although

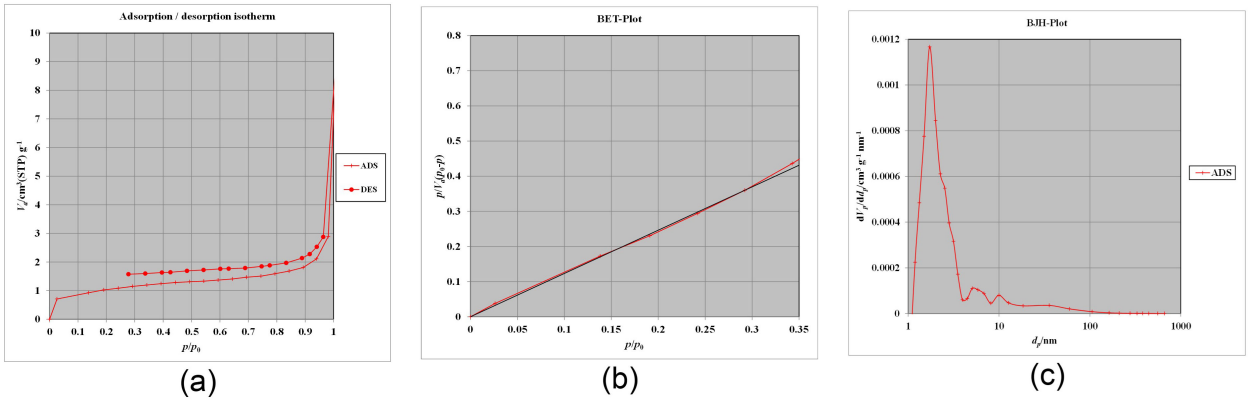

FIGURE 2
(a) N_2 adsorption/desorption isotherms, **(b)** BET surface area, and **(c)** BJH pore distribution confirming the mesoporous structure of the applied biochar.

surface area was low, the predominance of mesopores suggested functional capacity for water and nutrient interactions.

3.2 Soil nutrient retention and chemical properties

Biochar application significantly increased available N, Ca, and Mg ($p<0.05$), while pH, total N, total P, available P, and K remained largely unchanged. Soil parameters that significantly changed in response to biochar application are illustrated in Figure 3. Parameters with non-significant change in response to biochar application compared to control are presented in Supplementary Table 3. *A* slight increase in soil EC was observed due to higher Na and Cl concentrations.

Soil properties before and after biochar application are summarized in Table 1. Biochar caused a slight, non-significant reduction in bulk density, reflecting the lower density of biochar particles and their role in aggregation. More importantly, soil water content at both field capacity (Θ_{fc}) and permanent witling point (Θ_{PWP}) increased with biochar incorporation (Table 1). However, total available water (TAW) decreased, indicating that the observed increase in Θ_{fc} and Θ_{PWP} did not translate into greater plant-available water in this fine-textured soil. This finding suggests a shift toward finer mesopores that retain water too tightly to be available to plants. Such pore scale changes correspond with the depth-specific hydraulic conductivity response, where conductivity decreased in the upper 0–20 cm layer but increased in the 20–40 cm layer.

In the surface layer (0–20 cm), soil hydraulic conductivity was reduced from 1.23 cm h^{-1} in the control to 1.13 cm h^{-1} in the biochar-amended soils. On the contrary, the deeper layer (20–40 cm) observed an improvement in soil hydraulic conductivity in biochar amended soil (1.24 cm h^{-1}) compared to the control treatment (1.04 cm h^{-1}).

3.3 Soil water flux

The regression analysis revealed a strong significant relationship between measured SWC and TDR readings ($p<0.001$, 95% CL = 0.75–0.93, Figure 4). the calibration equation was derived as:

$$SWC = 6.84 + 0.505 \times TDR$$

This model explained 74% of the variance ($R^2 = 0.74$), with low prediction errors (RMSE = 6.4%, MAE = 5.0%). Diagnostic tests confirmed homoscedastic residuals (Breusch–Pagan p = 0.42) and only minor deviations from normality (Shapiro–Wilk p = 0.043). These results demonstrate that TDR provides a reliable proxy for SWC estimation in the studied soil profile.

Mean soil water fluxes are shown in Figure 5. The estimated marginal mean SWC values with their corresponding 95% confidence limits (CLs) are provided in Supplementary Table 4. Across both seasons, water fluxes were predominantly downward (negative values), consistent with drainage losses. Treatments differed significantly ($p<0.05$), and seasonal differences in drainage were dependent on treatment. Biochar combined with 80% nitrogen (B8) consistently minimized drainage, particularly in season 2, where losses were significantly lower (−0.012 cm d^{-1}, 95% CL: −0.025 to −0.001) compared with season 1 (−0.013 cm d^{-1}, 95% CL: −0.023 to 0.002). This indicates that moderate nitrogen supply optimized the soil–biochar interaction to reduce drainage losses under lower ET demand. Conversely, the B1 treatment exhibited greater drainage in season 1 (−0.034 cm d^{-1}, 95% CL: −0.044 to −0.023) than in season 2 (−0.021 cm d^{-1}, 95% CL: −0.035 to −0.008). The B5 treatment showed no significant seasonal variation. In contrast, the non-biochar treatments (W1, W5, and W8) exhibited minimal or statistically insignificant seasonal differences, indicating that the observed seasonal response was driven primarily by biochar–nitrogen interactions rather than irrigation regime alone.

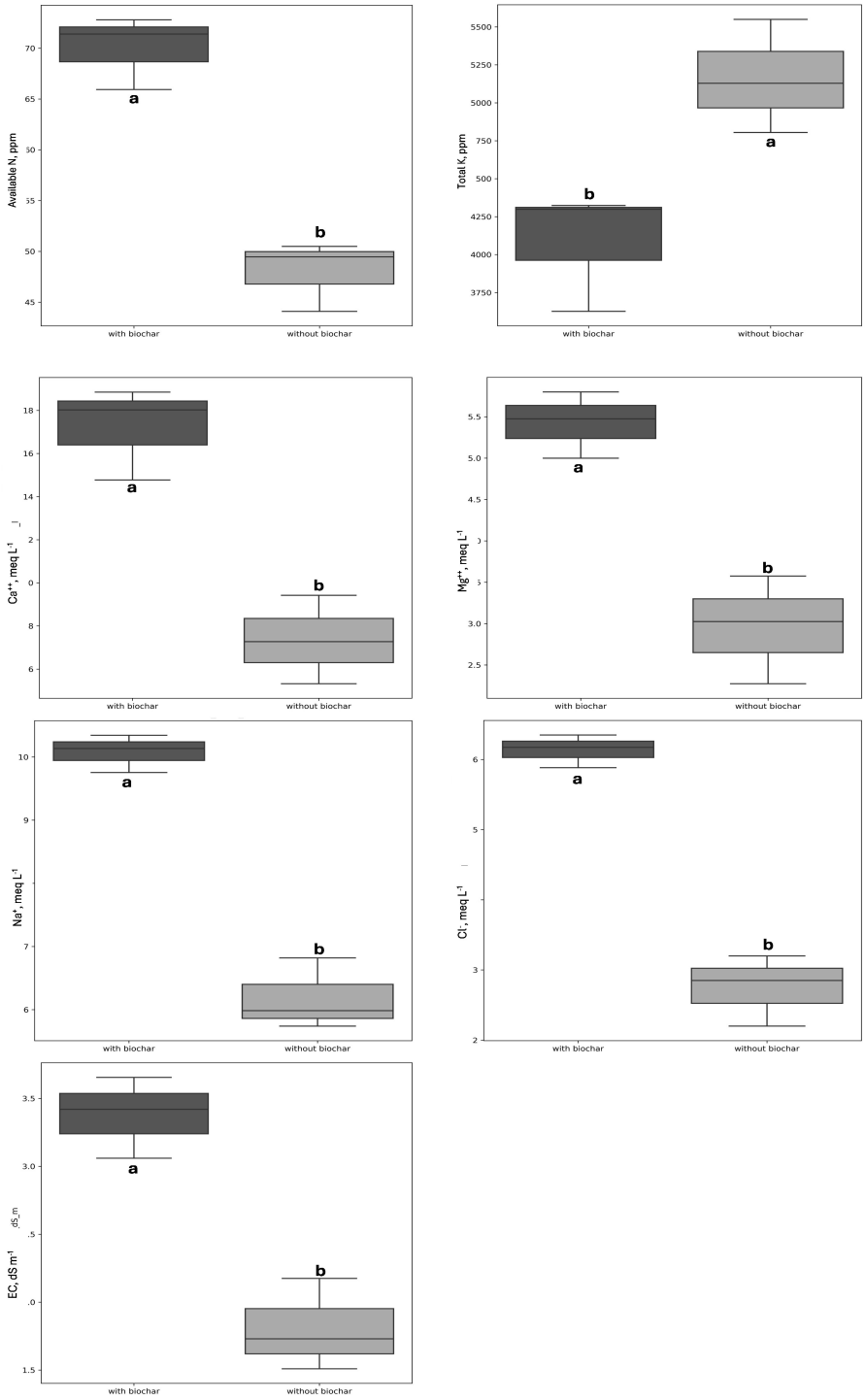

FIGURE 3
Soil nutrient concentrations and EC significantly affected by biochar compared with control ($p<0.05$).

3.4 Soil water content dynamics

Figure 6 illustrates vertical SWC distribution across soil depths in control and biochar-amended soils. Without biochar, SWC increased monotonically with depth, typical of shallow groundwater profiles. In contrast, biochar induced an S-shaped SWC profile, with greater retention in the 0–30 cm layer and a dip at 40 cm before rising again near the water table.

The interaction between treatments and soil depth is further shown in Figure 7. The estimated marginal mean (± standard error) of SWC under different combinations of biochar application and nitrogen levels is presented at Supplementary Table 4. Mixed-effects

TABLE 1 Soil properties (bulk density, Θ_{FC}, Θ_{PWP}, TAW, conductivity, pH, EC) before and after biochar application at 0–20 and 0–40 cm depths.

Treatment	Depth	SWC, % vol.			Hydraulic conductivity	Bulk density	pH	EC
	cm	Θ_{PWP}	Θ_{FC}	TAW	cm h^{-1}	g cm^{-3}		dS m^{-1}
With Biochar	0-20	20.35	41.90	21.55	1.13	1.30	7.90	3.66
	20-40	21.00	42.85	21.85	1.24	1.29	7.92	3.42
Without Biochar	0-20	15.35	41.15	25.80	1.23	1.35	7.72	2.18
	20-40	16.85	42.15	25.30	1.04	1.34	7.91	1.73

*SWC, soil water content, *θfc*, Soil water content at field capacity, and *θpwp*, Soil water content at permanent wilting point, TAW, total available water.

modeling confirmed a strong biochar × nitrogen interaction (F = 123, p< 0.0001). Among treatments, B8 exhibited the largest reduction in SWC relative to controls, particularly at intermediate depth (20–40 cm). This pattern highlights the capacity of biochar to reshape vertical water distribution even in shallow groundwater conditions. Model comparison further supported the inclusion of this interaction, as the depth–season interaction model (model 4) yielded the lowest AIC (10, 647.91) and BIC (10, 760.09), with a ΔAIC > 96 relative to the next best model (model 3), indicating strong support for model 4 as the best-fit structure (Supplementary Table 5). However, because irrigation replenished soil moisture to field capacity after each cycle, these hydrological adjustments influenced WUE rather than crop yield response.

3.5 Yield, quality, and irrigation water savings

Yield, fruit quality, and irrigation performance are summarized in Table 2. No statistically significant differences were detected across treatments. The absence of significant yield differences is consistent with the soil water flux and nutrient retention results, indicating that neither water availability nor nitrogen supply was limited under the experimental conditions. Although yield responses were muted, irrigation savings at scale could be agronomically and environmentally significant. The conventional practice of full irrigation and N fertilization (W1) was used as the baseline. The treatment B1 required the lowest irrigation volume (2435 m^3 ha^{-1}; WP = 36.75 kg m^{-3}), saving 82.43 m^3 ha^{-1} relative to W1, while maintaining a comparable fresh yield of 85, 174 kg ha^{-1}, with 1.88% below W1. By contrast, the W8 treatment achieved the highest fresh yield (105, 776 kg ha^{-1}; +21.85%) but required 23.80% more irrigation water, resulting in lower WP (35.50 kg m^{-3}), indicating reduced water use efficiency. A similar trend was observed for W5, which used 34.76% more irrigation water to achieve only a 12.01% yield increase (WP = 29.70 kg m^{-3}). This indicates that biochar's primary benefit under the present shallow groundwater and irrigation scheduling conditions was improved water productivity and use efficiency rather than yield productivity.

4 Discussion

4.1 Effects of biochar on soil nutrients and chemistry

The increase in available N, Ca, and Mg (Figure 3) can be attributed to biochar's inherent cation content and its surface functional groups that adsorb and retain cations (56, 57). Enhanced microbial activity in biochar amended soils may also contribute to N mineralization and cycling (58, 59).

Despite low BET surface area, biochar's mesoporous structure supports water and ion retention, which is especially relevant in fine textured soils. This highlights a surface area paradox: although high

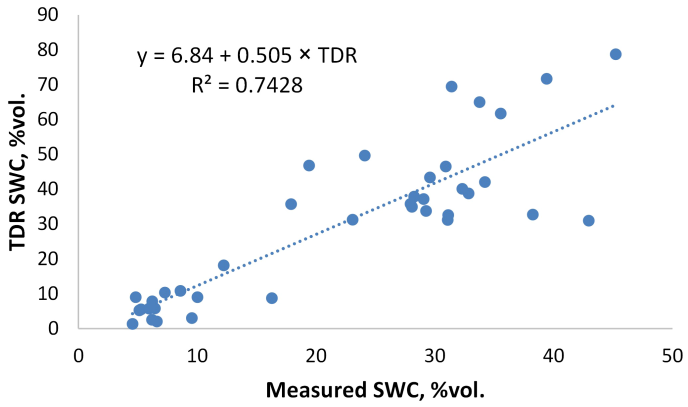

FIGURE 4
Relationship between measured SWC in the laboratory and TDR field measurements used for calibration.

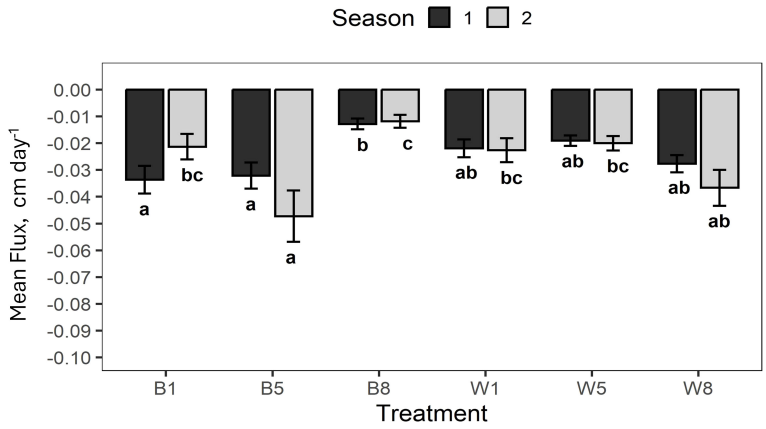

FIGURE 5
Mean soil water flux and standard error per treatment during the two seasons. Different lowercase letters indicate significant difference at $p<0.05$.

surface biochar enhances retention of larger molecules and nutrient via pore-filling and van der waals forces (60, 61). Thus, even low-surface-area biochar can be effective if mesoporosity dominates its structure.

4.2 Soil water retention and hydraulic changes

The observed increase in θ_{fc} and θ_{pwp} (Table 1) aligns with studies reporting improved retention at specific matric potentials under biochar (62, 63). However, the concurrent reduction in TAW reflects the interaction of biochar with fine-textured soils, where high inherent water-holding capacity may be disrupted (10, 64).

Reduced hydraulic conductivity in the topsoil but increased conductivity at 20–40 cm (Table 1) suggests redistribution of flow pathways (65). Specifically, biochar incorporation in the surface layer (0–20 cm) likely reduced macropore continuity by partially filling or bridging larger pores, thereby slowing vertical water movement near the surface. Meanwhile, percolating dissolved biochar particles may have enhanced aggregation and pore connectivity at 20–40 cm, facilitating preferential percolation pathways at depth. These findings indicate that biochar modifies not only soil water holding capacity but also the depth-specific balance between retention and conductivity.

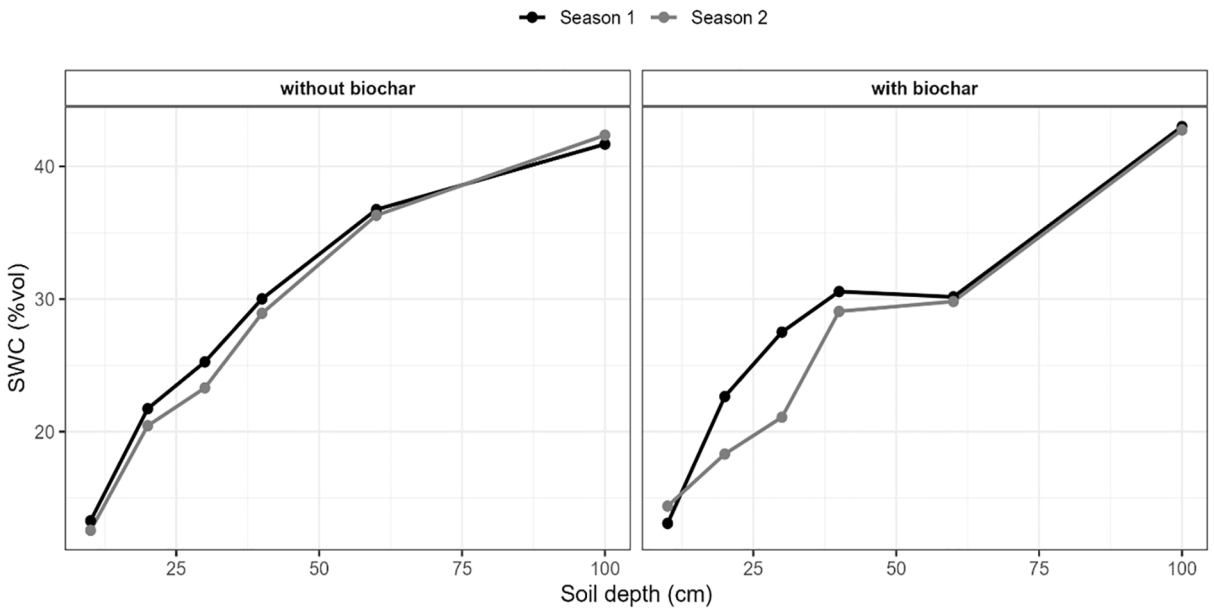

FIGURE 6
Vertical distribution of volumetric soil SWC (%vol.) across soil depths in control (left) and biochar-amended soils (right) for two seasons. Shaded bands represent 95% confidence intervals.

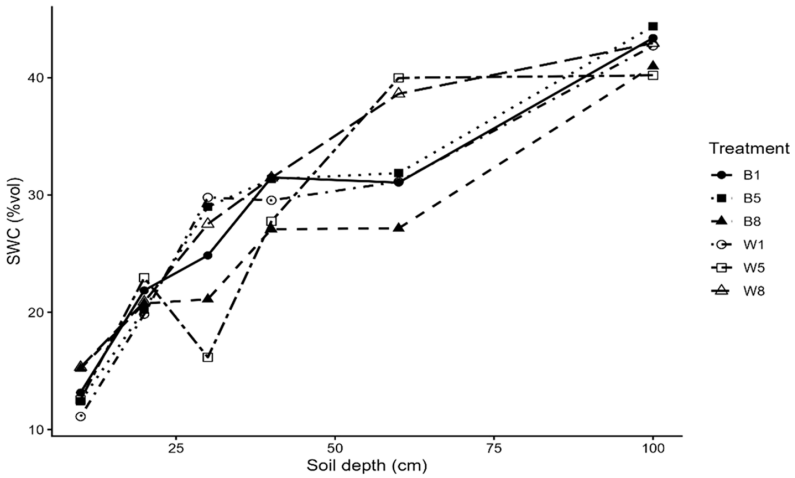

FIGURE 7
Interaction between biochar–nitrogen treatments and soil depth on mean SWC (%vol) across the study period.

The observed reduction in TAW, despite increase in both θ_{fc} and θ_{pwp}, likely reflects a shift toward water being retained in finer pores where it is held at higher matric tension and therefore less available to plants. In fine-textured soils, biochar particles can occupy or partially occlude inter-aggregate macropores, reducing pore continuity and promoting water retention in smaller pores – a process often described as pore clogging (12, 13). This aligns with our finding that hydraulic conductivity decreased in the 0–20 cm layer where biochar was incorporated. In contrast, the increase in conductivity observed at 20–40 cm suggests improved pore connectivity at depth, consistent with reports that organic amendments promote subsoil structural development and preferential flow channel stabilization in fine textured soils (15). Thus, the redistribution of flow pathways is characterized by reduced near-surface hydraulic transmission and enhanced deeper percolation channels. These findings suggest that biochar application in clay loam soils should be carefully managed to avoid reduction in plant-available water in the surface layer, possibly by adjusting application depth or combining with structure promoting soil amendments. These contrasting depth-specific responses highlight that biochar does not uniformly increase soil hydraulic function but instead redistributes water retention and flow pathways within the profile.

4.3 Water flux and vertical soil moisture profiles

The S-shaped SWC distribution under biochar (Figures 5, 6) contrasts with the monotonic profile of unamended soil with biochar and reveals a shift in soil water dynamics. This agrees with (66), who found enhanced SWC in biochar–N combinations within the root zone. In the upper 0–20 cm, biochar incorporation enhanced water retention, resulting in higher near-surface SWC. The middle layer (20–40 cm) exhibited a relative plateau or local minimum SWC, indicating reduced downward transmission through this zone. Below 60 cm, SWC increased again, reflecting the influence of the shallow groundwater table and capillary return.

This pattern differs from biochar effects in free draining soils, where deeper percolation often increases SWC at depth due to

TABLE 2 Irrigation volume, fresh yield, water productivity, water savings, and fruit quality parameters (TSS, moisture, lycopene) ± standard error for all treatments.

Treatment	Applied irrigation	Fresh yield	WP	Water saving[1]	TSS	Moisture content	Lycopene
	m^3 ha^{-1}	Kg ha^{-1}	Kg m^{-3}	m^3 ha^{-1}	%	%	mg $100g^{-1}$
B1	2435 ± 351	85174 ± 9533	36.75 ± 5.27	82.43	4.28 ± 0.14	94.96 ± 0.23	15.72 ± 2.64
B8	2602 ± 358	95902 ± 9523	41.76 ± 8.89	−84.74	4.35 ± 0.06	94.84 ± 0.20	17.01 ± 2.58
B5	2503 ± 232	99077 ± 3587	41.92 ± 5.13	14.53	4.23 ± 0.11	95.12 ± 0.19	17.76 ± 2.30
W1	2517 ± 318	86810 ± 9271	37.63 ± 8.80	baseline	4.15 ± 0.05	95.03 ± 0.16	19.97 ± 1.27
W8	3116 ± 365	105776 ± 8109	35.50 ± 4.56	−598.96	4.24 ± 0.12	95.19 ± 0.71	20.17 ± 1.57
W5	3392 ± 431	97238 ± 23376	29.70 ± 7.99	−874.26	4.2 ± 0.15	95.24 ± 0.15	19.65 ± 1.07

[1]Water saving (mean) indicates the absolute reduction in applied water compared with the baseline, positive values indicate water savings, negative values indicate higher water use. Where WP: water productivity, TSS: total soluble solids.

unrestricted drainage (39). In contrast, in our shallow-groundwater setting, limited vertical drainage and upward capillary feedback produce an S-shaped moisture structure driven by retention above and re-wetting below the root zone.

Across seasons, the B8 treatment reduced downward flux by approximately 0.010–0.022 cm d^{-1} relative to the control (Supplementary Table 4). Corresponding to a reduction of about 30–45% in drainage losses. This redistribution supports greater water availability within the primary rooting zone, which may be advantageous in shallow groundwater systems where managing vertical water distribution is more critical than maximizing total storage.

4.4 Crop response and irrigation water savings

Although yield and fruit quality responses were statistically non-significant (Table 2), numerical differences are meaningful under water-scarce conditions. As discussed in Section 4.2, the reduction in TAW was mainly associated with water held at higher matric tension in finer pores, while plant-available water in the effective root zone remained sufficient due to shallow groundwater buffering. Similar inconsistencies in biochar yield responses have been reported, with stronger effects in nutrient-poor or coarse soils (67–69). In the present study the shallow groundwater table may have partially moderated treatment differences by contributing supplementary moisture through capillary rise. While upward fluxes were not directly quantified and downward drainage remained the dominant flux pathway, the consistent presence of groundwater within the capillary influence zone can buffer crop water stress and help explain the muted yield response (70, 71). In addition, further studies reported that shallow groundwater, waterlogging and reduced aeration may attenuate yield benefits (20, 72).

Nevertheless, the irrigation savings observed in B1 (Table 2) highlight biochar's potential for improving water productivity without compromising yields. This aligns with recent studies demonstrating that biochar can increase soil water retention and improve WUE in clay and clay loam soils (73, 74). When extrapolated to Egypt's tomato cultivation area of 990, 476 ha (75), this corresponds to approximately 65.3 to 81.6 million m^3 yr^{-1} of water saved assuming 80% and 100% irrigation efficiency, respectively under similar hydrological and environmental conditions. Extending this to the MENA region, where tomato cultivation covers 1, 414, 057 ha (76), the savings could reach about 92.8–116 million m^3 yr^{-1}. Although the per-hectare savings may appear modest, their cumulative regional impact highlights a significant opportunity for improved water resources management even under conservative efficiency scenarios, with no yield penalties.

However, these regional estimates should be interpreted with caution, as soil texture groundwater depth, and irrigation practices vary widely across the MENA region. Multi-site field validation under constructing agro-hydrological settings would be necessary to confirm the scalability of the observed biochar–water interaction and to refine region-specific recommendation.

4.5 Implications and future research

These results confirms that biochar–N interactions extend beyond nutrient cycling to hydrological regulation. By reshaping soil moisture profiles (Figures 5, 6), biochar offers a mechanism to adapt irrigation in regions where shallow groundwater interacts with agriculture. Long-term trials and modelling are needed to capture cumulative effects and to evaluate interactions under variable climate and cropping systems.

5 Conclusions

This study demonstrates that biochar with a mesoporous structure can substantially modify soil hydrology under shallow groundwater conditions. Biochar increased soil water retention at field capacity and wilting point and, more importantly, reshaped the vertical soil moisture profile, creating an S-shaped distribution distinct from the conventional pattern. These effects were most evident in the incorporation zone (0–30 cm) and were amplified when combined with full or moderate nitrogen fertilization.

While short-term effects on tomato yield and quality were limited, the biochar + full nitrogen treatment reduced irrigation demand without compromising production, highlighting its potential for improving water productivity. Extrapolation of these results indicates that modest field-level savings can translate into substantial regional water conservation across Egypt and MENA region.

Overall, mesoporous biochar integrated with nitrogen management offers a soil-based strategy to regulate water dynamics under shallow groundwater, providing both hydrological and agronomic benefits. Long-term trials and mechanistic modelling are needed to further elucidate biochar's role in enhancing soil–water functions under diverse pedoclimatic conditions.

Data availability statement

The datasets presented in this study can be found in online repositories. The names of the repository/repositories and accession number(s) can be found in the article/Supplementary Material.

Author contributions

ME: Conceptualization, Data curation, Formal Analysis, Investigation, Methodology, Resources, Software, Validation, Visualization, Writing – original draft, Writing – review & editing. RG: Conceptualization, Investigation, Methodology, Writing – review & editing. ME-S: Conceptualization, Investigation, Methodology, Visualization, Writing – review & editing. MR: Methodology, Writing – review & editing. YB:

Methodology, Visualization, Writing – review & editing. AA: Conceptualization, Funding acquisition, Investigation, Methodology, Project administration, Supervision, Writing – review & editing.

Funding

The author(s) declare that financial support was received for the research and/or publication of this article. This research was funded by the Egyptian Academy of Scientific Research and Technology (ASRT) under the Climate Change Action Plan (COP27 and Beyond Program, SAM-EGY).

Acknowledgments

The authors express their sincere appreciation to the Arid Land and Agriculture Research Institute (ALARI), Ain Shams University, Egypt, for their invaluable support throughout the experimental phase of this study. The Institute's provision of essential equipment and timely access to relevant data significantly contributed to the successful execution of the research.

Conflict of interest

The authors declare that the research was conducted in the absence of any commercial or financial relationships that could be construed as a potential conflict of interest.

Generative AI statement

The author(s) declare that Generative AI was used in the creation of this manuscript. During the preparation of this manuscript, the authors used Microsoft 365 Copilot to enhance the quality of writing and to correct grammatical and linguistic errors. The authors have thoroughly reviewed and edited the content and take full responsibility for the final version of this publication.

Any alternative text (alt text) provided alongside figures in this article has been generated by Frontiers with the support of artificial intelligence and reasonable efforts have been made to ensure accuracy, including review by the authors wherever possible. If you identify any issues, please contact us.

Publisher's note

Supplementary material

The Supplementary Material for this article can be found online at: https://www.frontiersin.org/articles/10.3389/fsoil.2025.1718929/full#supplementary-material

References

1. Abujabhah IS, Bound SA, Doyle R, Bowman JP. Effects of biochar and compost amendments on soil physico-chemical properties and the total community within a temperate agricultural soil *Appl Soil Ecol*. (2016) 98:243–253. doi: 10.1016/j.apsoil.2015.10.021

2. Belmonte BA, Benjamin MFD, Tan RR. Biochar systems in the water-energy-food nexus: the emerging role of process systems engineering *Curr Opin Chem Eng*. (2017) 18:32–37. doi: 10.1016/j.coche.2017.08.005

3. Abbas A, Hameed R, Shahani AAA, Khattak WA, Huang P, Du D. Biochar mediated carbon and nutrient dynamics under arable land. *Biochar Production for Green Economy*. (2024), 161–184. doi: 10.1016/B978-0-443-15506-2.00024-9

4. Gunasekaran PK, Chin SC. Performance of bamboo biochar as partial cement replacement in mortar *Mater Today Proc*. (2024) 109:53–61. doi: 10.1016/j.matpr.2023.06.322

5. Moussa LG, Mohan M, Pitumpe Arachchige PS, Rathnasekara H, Abdullah M, Jaffar A, et al. Impact of water availability on food security in GCC: Systematic literature review-based policy recommendations for a sustainable future *Environ Dev*. (2025) 54:1–17. doi: 10.1016/j.envdev.2024.101122

6. Yan S, Niu Z, Zhang A, Yan H, Zhang H, He K, et al. Biochar application on paddy and purple soils in southern China: soil carbon and biotic activity . *R Soc Open Sci*. (2019) 6:1–16. doi: 10.1098/rsos.181499

7. Gonçalves MAF, da Silva BRS, Nobre JRC, Batista BL, da Silva Lobato AK. Biochar mitigates the harmful effects of drought in soybean through changes in leaf development, stomatal regulation, and gas exchange *J Soil Sci Plant Nutr*. (2024) 24:1940–51. doi: 10.1007/s42729-024-01663-7

8. Obadi A, Alharbi A, Alomran A, Alghamdi AG, Louki I, Alkhasha A, et al. Enhancement in tomato yield and quality using biochar amendments in greenhouse under salinity and drought stress *Plants*(2024) 13:1634. doi: 10.3390/plants13121634

9. Umer S, Akram NA, Bukhari I, Abdel Latef AAH. Biochar for alleviation of salinity stress in plants. *Biochar in Mitigating Abiotic Stress in Plants*. (2025), 173–192. doi: 10.1016/B978-0-443-24137-6.00011-2

10. Wei B, Peng Y, Lin L, Zhang D, Ma L, Jiang L, et al. Drivers of biochar-mediated improvement of soil water retention capacity based on soil texture: A meta-analysis *Geoderma* (2023) 437:116591. doi: 10.1016/j.geoderma.2023.116591

11. Majumder D, Fahad S, Hossain A. Biochar versus soil health under changing climate. *Biochar-assisted Remediation of Contaminated Soils Under Changing Climate*. Amsterdam: Elsevier Inc. (2024), 35–69. doi: 10.1016/B978-0-443-21562-9.00002-5.

12. Saifullah D, Naeem A, Rengel ZA, Naeem A. Biochar application for the remediation of salt-affected soils: Challenges and opportunities *Sci Total Environ*. (2018) 625:320–335. doi: 10.1016/j.scitotenv.2017.12.257

13. Mansour Shahsavar A, Mosaddeghi MR, Rahimmalek M, Gheysari M. Interactive effects of wood biochar application and Thymus species on soil physical quality in irrigated farming *Soil Tillage Res*. (2024) 244. doi: 10.1016/j.still.2024.106260

14. Jiang RW, Mechler MA, Oelbermann M. Exploring the effects of one-time biochar application with low dosage on soil health in temperate climates *Soil Secur*. (2023) 12:1–10. doi: 10.1016/j.soisec.2023.100101

15. Qi S, Degen AA, Guo R, Rafiq MK, Shang Z. Biochar utilization for alpine grassland restoration. *Grassland Degradation, Restoration and Sustainable Management of Global Alpine Area*. (2025), 325–341. doi: 10.1016/B978-0-443-21882-8.00015-9

16. Fan Y, Li H, Miguez-Macho G. Global patterns of groundwater T able depth *Science*. (2013) 339:940–3. doi: 10.1126/science.1229881

17. Rong Y, Dai X, Wang W, Wu P, Huo Z. Dependence of evapotranspiration validity on shallow groundwater in arid area-a three years field observation experiment *Agric Water Manag*. (2023) 286:1–14. doi: 10.1016/j.agwat.2023.108411

18. Zhu Y, Zhao T, Mao W, Ye M, Han X, Jia B, et al. Development of flow model for partly and fully saturated soils using water balance and water ta ble depth fluctuation analysis *J Hydrol (Amst)*. (2023) 618:1–17. doi: 10.1016/j.jhydrol.2023.129259

19. Khan S, Rana T, Hanjra MA, Zirilli J. Water markets and soil salinity nexus: Can minimum irrigation intensities address the issue? *Agric Water Manag*. (2009) 96:493–503. doi: 10.1016/j.agwat.2008.09.014

20. Florio EL, Mercau JL, Jobbágy EG, Nosetto MD. Interactive effects of water-t able depth, rainfall variation, and sowing date on maize production in the Western Pampas *Agric Water Manag*. (2014) 146:75–83. doi: 10.1016/j.agwat.2014.07.022

21. Rizzo G, Edreira JIR, Archontoulis SV, Yang HS, Grassini P. Do shallow water ta bles contribute to high and sta ble maize yields in the US Corn Belt? *Glob Food Sec*. (2018) 18:27–34. doi: 10.1016/j.gfs.2018.07.002

22. Florio EL, Nosetto MD. A modeling approach to explore the influence of different crop rotations on water-ta ble depths and crop yields in the Pampas *Soil Tillage Res*. (2022) 223:1–12. doi: 10.1016/j.still.2022.105496

23. Videla-Mensegue H, Magra MS, Macchiavello A, Álvarez C, Noellemeyer E, Caviglia OP. (2025). doi: 10.1016/j.geodrs.2025.e00956

24. Fernández-Cirelli A, Arumí JL, Rivera D, Boochs PW. Environmental effects of irrigation in arid and semi-arid regions *Chil J Agric Res*. (2009) 69:27–40. doi: 10.4067/s0718-58392009000500004

25. Mahmoud MA. Groundwater and agriculture in the nile delta In: *Handbook of environmental chemistry*. Heidelberg: Springer Verlag (2019). p. 141–57. doi: 10.1007/698_2017_94

26. Shao G, Gao Y, Lin J, Liu Z, Huang D. Effects of Biochar on Water Requirement Regulation and Yield of Tomato under Different Groundwater Tab les *Nongye Jixie Xuebao/Transactions Chin Soc Agric Machinery*. (2019) 50:250–258. doi: 10.6041/j.issn.1000-1298.2019.11.028

27. Zhang K, Shao G, Wang Z, Cui J, Lu J, Gao Y. Modeling the impacts of groundwater depth and biochar addition on tomato production under climate change using RZWQM2 *Sci Hortic*. (2022) 302:1–16. doi: 10.1016/j.scienta.2022.111147

28. Du Y-D, Niu W-Q, Gu X-B, Zhang Q, Cui B-J. Water- and nitrogen-saving potentials in tomato production: A meta-analysis *Agric Water Manag*. (2018) 210:296–303. doi: 10.1016/j.agwat.2018.08.035

29. Wu Y, Yan S, Fan J, Zhang F, Zheng J, Guo J, et al. Combined application of soluble organic and chemical fertilizers in drip fertigation improves nitrogen use efficiency and enhances tomato yield and quality *J Sci Food Agric*. (2020) 100:5422–5433. doi: 10.1002/jsfa.10593

30. Zeleke YG, Haile A, Kiflu A, Alemayehu H. Morphological and physiological plasticity of tomato in response to Azolla fern, a novel organic fertilizer of environmentally friendliness *Heliyon*. (2024) 10:1–10. doi: 10.1016/j.heliyon.2024.e39110

31. Du YD, Zhang Q, Cui BJ, Sun J, Wang Z, Ma LH, et al. Aerated irrigation improves tomato yield and nitrogen use efficiency while reducing nitrogen application rate *Agric Water Manag*. (2020) 235:1–11. doi: 10.1016/j.agwat.2020.106152

32. Li H, Liu H, Gong X, Li S, Pang J, Chen Z, et al. Optimizing irrigation and nitrogen management strategy to trade off yield, crop water productivity, nitrogen use efficiency and fruit quality of greenhouse grown tomato *Agric Water Manag*. (2021) 245:1–11. doi: 10.1016/j.agwat.2020.106570

33. Hagemann N, Harter J, Behrens S. *Elucidating the impacts of biochar applications on nitrogen cycling microbial communities*. Amesterdam: Elsevier (2016). doi: 10.1016/B978-0-12-803433-0.00007-2.

34. Gu S, Lian F, Yang H, Han Y, Zhang W, Yang F, et al. Synergic effect of microorganism and colloidal biochar-based organic fertilizer on the growth and fruit quality of tomato *Coatings*. (2021) 11:1–11. doi: 10.3390/coatings11121453

35. Abdelghany AE, Dou Z, Alashram MG, Eltohamy KM, Elrys AS, Liu X, et al. The joint application of biochar and nitrogen enhances fruit yield, quality and water-nitrogen productivity of water-stressed greenhouse tomato under drip fertigation . *Agric Water Manag*. (2023) 290:1–15. doi: 10.1016/j.agwat.2023.108605

36. Kohira Y, Fentie D, Lewoyehu M, Wutisirirattanachai T, Gezahegn A, Addisu S, et al. Elucidation of ammonium and nitrate adsorption mechanisms by water hyacinth biochar: effects of pyrolysis temperature *Environ Sci pollut Res*. (2024) 32:762–82. doi: 10.1007/s11356-024-35808-z

37. Wei B, Peng Y, Lin L, Zhang D, Ma L, Jiang L, et al. Drivers of biochar-mediated improvement of soil water retention capacity based on soil texture: A meta-analysis *Geoderma*. (2023) 437:1–11. doi: 10.1016/j.geoderma.2023.116591

38. Cao J, Jiang Y, Tan X, Li L, Cao S, Dou J, et al. Sludge-based biochar preparation: pyrolysis and co-pyrolysis methods, improvements, and environmental applications *Fuel*. (2024) 373:1–17. doi: 10.1016/j.fuel.2024.132265

39. Jiang Z, Huang S, Meng Z. Long-term effects of biochar on the hydraulic properties of soil: A meta -analysis based on 1–10 years field experiments *Geoderma*. (2025) 458:458. doi: 10.1016/j.geoderma.2025.117318

40. Guo L, Yu H, Kharbach M, Zhang W, Wang J, Niu W. Biochar improves soil-tomato plant, tomato production, and economic benefits under reduced nitrogen application in northwestern China . *Plants*. (2021) 10:1–15. doi: 10.3390/plants10040759

41. Irwansyah FS, Amal AI, Diyanthi EW, Hadisantoso EP, Noviyanti AR, Eddy DR, et al. How to read and determine the specific surface area of inorganic materials using the brunauer-emmett-teller (BET) method *ASEAN J Sci Eng*. (2024) 4:61–70. doi: 10.17509/ajse.v4i1.60748

42. Savva AP, Frenken K. *Irrigation Manual Module 4 Crop Water Requirements and Irrigation Sched uling Developed by. Harare* (2002). FAO Sub-Regional Office for East and Southern Africa. Available online at: https://openknowledge.fao.org/server/api/core/bitstreams/e7d053e8-9c16-4ceb-80d5-990865b794c6/content (Accessed November 27, 2025).

43. Estefan G, Sommer R, Ryan J. *Methods of Soil, Plant, and Water Analysis: A manual for the West Asia and North Africa region*. (2013). Beirut: International Center for Agricultural Research in the Dry Areas (ICARDA. Available online at: https://repo.mel.cgiar.org/items/14bb2a3f-dc9e-455b-99e3-97f27ceb9e42 (Accessed November 27, 2025).

44. Chapman HD, Pratt PF. Methods of analysis for soils, plants and waters *Soil Sci*. (1962) 93:1–309. doi: 10.1097/00010694-196201000-00015

45. Sadler G, Davis J, Dezman D. Rapid extraction of lycopene and β-carotene from reconstituted tomato paste and pink grapefruit homogenates *J Food Sci*. (1990) 55:1460–1461. doi: 10.1111/j.1365-2621.1990.tb03958.x

46. Cottenie A. Soil and plant testing and analysis as a basis of fertilizer recommendations In: *FAO soils bulletin no. 38/2*. Rome: Food and Agriculture Organization of the United Nations (FAO) (1980). p. 119.

47. Westerman RL. (2018). doi: 10.2136/sssabookser3.3ed

48. Elbana M. Dataset for Mesoporous biochar reshapes soil water dynamics under shallow groundwater: interactions with nitrogen management. *Zenodo* (2025). doi: 10.5281/zenodo.17195601

49. Black CA. *Methods of Soil Analysis: Part 1 Physical and mineralogical properties, including statistics of measurements and sampling,*. Black. Madison CA, editor. WI, USA: American Society of Agronomy, Soil Science Society of America (1965). doi: 10.2134/agronmonogr9.1

50. Rees SW, Adjali MH, Zhou Z, Davies M, Thomas HR.). Ground heat transfer effects on the thermal performance of earth-contact structures *Renewable Sustain Energy Rev*. (2000) 4:213–265. doi: 10.1016/S1364-0321(99)00018-0

51. Rolston DE. Historical development of soil-water physics and solute transport in porous media *Water Supply*. (2007) 7:59–66. doi: 10.2166/ws.2007.007

52. van Genuchten M. A closed-form equation for predicting the hydraulic conductivity of unsaturated soils *Soil Sci Soc America J*. (1980) 44:892–8. doi: 10.2136/sssaj1980.03615995004400050002x

53. Mualem Y. A new model for predicting the hydraulic conductivity of unsaturated porous media *Water Resour Res*. (1976) 12:513–22. doi: 10.1029/WR012i003p00513

54. Steduto P, Hsiao TC, Fereres E, Raes D. Crop yield response to water In: *FAO irrigation and drainage paper*. Rome: Food and Agriculture Organization of the United Nations (FAO) (2012). p. 66.

55. Thommes M, Kaneko K, Neimark AV, Olivier JP, Rodriguez-Reinoso F, Rouquerol J, et al. Physisorption of gases, with special reference to the evaluation of surface area and pore size distribution (IUPAC Technical Report) *Pure Appl Chem*. (2015) 87:1051–1069. doi: 10.1515/pac-2014-1117

56. Ji M, Sang W. The remediation potential of biochar derived from different biomass for typical pollution in agricultural soil. *Biochar in Agriculture for Achieving Sustainable Development Goals*. Amesterdam: Elsevier (2022). doi: 10.1016/B978-0-323-85343-9.00017-3.

57. Ramesh K, Raghavan V. Biochar/bentonite composite beads for controlled nitrogen release and reduced environmental impact: From banana waste to sustainable food security *Results Surfaces Interfaces*. (2025) 19:1–10. doi: 10.1016/j.rsurfi.2025.100500

58. Guan R, Li Y, Jia Y, Jiang F, Li L, Biswas A, et al. Dual impact of single acidified biochar application on saline-alkaline soil: short-term salinization risks and persistent nutrient benefits *Soil Tillage Res*. (2025) 254:1–19. doi: 10.1016/j.still.2025.106745

59. Rehali M, El Ghachtouli N, Lange SF, Bouamri R. Valorization of date palm residues for biochar production: Assessing biochar characteristics for agricultural application *Sci Afr*. (2025) 27:1–16. doi: 10.1016/j.sciaf.2025.e02599

60. Saghir S, Pu C, Fu E, Wang Y, Xiao Z. Synthesis of high surface area porous biochar obtained from pistachio shells for the efficient adsorption of organic dyes from polluted water *Surfaces Interfaces*. (2022) 34:1–12. doi: 10.1016/j.surfin.2022.102357

61. Ihsanullah I, Bilal M, Khan U, Zulfiqar R, Ali S, Khan MT. Biochar as a sustainable solution for per- and polyfluoroalkyl substances (PFAS) Removal: Progress, Challenges, and Future Horizons *Sep Purif Technol*. (2025) 365:1–18. doi: 10.1016/j.seppur.2025.132674

62. Fischer BMC, Manzoni S, Morillas L, Garcia M, Johnson MS, Lyon SW. Improving agricultural water use efficiency with biochar – A synthesis of biochar effects on water storage and fluxes across scales *Sci Total Environ*. (2019) 657:853–862. doi: 10.1016/j.scitotenv.2018.11.312

63. Yang CD, Lu SG. Effects of five different biochars on aggregation, water retention and mechanical properties of paddy soil: A field experiment of three-season crops *Soil Tillage Res*. (2021) 205:1–11. doi: 10.1016/j.still.2020.104798

64. Zhang J, Amonette JE, Flury M. Effect of biochar and biochar particle size on plant-available water of sand, silt loam, and clay soil *Soil Tillage Res*. (2021) 212:104992. doi: 10.1016/j.still.2021.104992

65. Castellini M, Giglio L, Niedda M, Palumbo AD, Ventrella D. Impact of biochar addition on the physical and hydraulic properties of a clay soil *Soil Tillage Res*. (2015) 154:1–13. doi: 10.1016/j.still.2015.06.016

66. Yeboah S, Zhang R, Cai L, Li L, Xie J, Luo Z, et al. Soil water content and photosynthetic capacity of spring wheat as affected by soil application of nitrogen-enriched biochar in a semiarid environment *Photosynthetica*. (2017) 55:532–42. doi: 10.1007/s11099-016-0672-1

67. Arif M, Ilyas M, Riaz M, Ali K, Shah K, Ul Haq I, et al. Biochar improves phosphorus use efficiency of organic-inorganic fertilizers, maize-wheat productivity and soil quality in a low fertility alkaline soil *Field Crops Res*. (2017) 214:25–37. doi: 10.1016/j.fcr.2017.08.018

68. Meng F, Yang H, Fan X, Gao X, Tai J, Sa R, et al. A microbial ecosystem enhanced by regulating soil carbon and nitrogen balance using biochar and nitrogen fertiliser five years after application *Sci Rep*. (2023) 13:22233. doi: 10.1038/s41598-023-49140-y

69. Sun X, Yang X, Hu Z, Liu F, Xie Z, Li S, et al. Biochar effects on soil nitrogen retention, leaching and yield of perennial citron daylily under three irrigation regimes *Agric Water Manag*. (2024) 296:1–9. doi: 10.1016/j.agwat.2024.108788

70. Chen S, Mao X, Shang S. Response and contribution of shallow groundwater to soil water/salt budget and crop growth in layered soils *Agric Water Manag*. (2022) 266:107574. doi: 10.1016/j.agwat.2022.107574

71. Gao X, Huo Z, Qu Z, Tang P. Modeling agricultural hydrology and water productivity to enhance water management in the arid irrigation district of China In: *Enhancing agricultural research and precision management for subsistence farming by integrating system models with experiments*. American Society of Agronomy (ASA), Crop Science Society of America (CSSA), and Soil Science Society of America (SSSA) (2022). doi: 10.1002/9780891183891.ch6

72. Jeffery S, Meinders MBJ, Stoof CR, Bezemer TM, van de Voorde TFJ, Mommer L, et al. Biochar application does not improve the soil hydrological function of a sandy soil *Geoderma*. (2015) 251–252:47–54. doi: 10.1016/j.geoderma.2015.03.022

73. Esmaeilnezhad R, Zeinalzadeh K, Besharat S, Kheirfam H. Field study on the hydraulic behavior of heavy soil: Effects of biochar application rates *Sci Total Environ*. (2025) 1004:180752. doi: 10.1016/j.scitotenv.2025.180752

74. Ouyang Z, Zhang J, Liang X, Wang H, Yang Z, Tang R, et al. Micro-nano aerated subsurface drip irrigation and biochar promote photosynthesis, dry matter accumulation and yield of cucumbers in greenhouse *Agric Water Manag*. (2025) 308:109295. doi: 10.1016/j.agwat.2025.109295

75. CAPMAS. (2024). *Statistical Year Book 2024*Cairo: Central Agency for Publich Mobilization and Statistics. Available online at: https://www.capmas.gov.eg/pages/staticpages.aspx?page_id=5034 (Accessed August 15, 2025).

76. FAO. *FAOSTAT: crops and livestock products*. (2023). Food and Agriculture Organization of the United Nations. Available online at: https://www.fao.org/faostat/en/data/QCL (Accessed August 28, 2025).